Swansea University
Prifysgol Abertawe

Cronfa
Setting Research Free

Cronfa - Swansea University Open Access Repository

_____

This is an author produced version of a paper published in:
Electrocatalysis

_____

Cronfa URL for this paper:
http://cronfa.swan.ac.uk/Record/cronfa47963

_____

Paper:

Ganesan, V., Madrid, E., Malpass-Evans, R., Carta, M., McKeown, N. & Marken, F. (2018). Biphasic Voltammetry and Spectroelectrochemistry in Polymer of Intrinsic Microporosity—4-(3-Phenylpropyl)-Pyridine Organogel/Aqueous Electrolyte Systems: Reactivity of MnPc Versus MnTPP. *Electrocatalysis*

http://dx.doi.org/10.1007/s12678-018-0497-8

_____

http://www.swansea.ac.uk/library/researchsupport/ris-support/

ORIGINAL RESEARCH

CrossMark

Biphasic Voltammetry and Spectroelectrochemistry in Polymer of Intrinsic Microporosity—4-(3-Phenylpropyl)-Pyridine Organogel/Aqueous Electrolyte Systems: Reactivity of MnPc Versus MnTPP

Vellaichamy Ganesan[1,2] · Elena Madrid[1] · Richard Malpass-Evans[3] · Mariolino Carta[4] · Neil B. McKeown[3] · Frank Marken[1]

Abstract

A hydrophobic polymer of intrinsic microporosity (PIM-EA-TB) is employed to stabilize an organogel/aqueous electrolyte phase boundary based on an organic water-insoluble 4-(3-phenylpropyl)-pyridine phase. The organogel with electrocatalytic metal complexes embedded is immobilized on glassy carbon or on transparent mesoporous tin-doped indium oxide (ITO) electrodes. Liquid/liquid ion transfer voltammetry is investigated for a 4-(3-phenylpropyl)-pyridine organogel/aqueous electrolyte interface for two types of redox systems: tetraphenylporphyrinato-Mn(III/II) (MnTPP) and phthalocyanato-Mn(III/II) (MnPc). Electron transfer is shown to be coupled to reversible liquid/liquid anion transfer processes for PF_6^-, ClO_4^-, SCN^-, and NO_3^-, with a change in mechanism for the more hydrophilic anions Cl^-, F^-, and SO_4^{2-}. In situ UV-Vis spectroelectrochemistry reveals reversible Mn(III/II) redox processes coupled to ion transfer for MnTPP. But further complexity and a detrimental side reaction are observed for MnPc causing gradual loss of the electrochemical response in the presence of dioxygen.

Keywords Voltammetry · Electrochromic · Anion transfer · Catalysis · Microporosity · Sensor

Introduction

Liquid/liquid ion transfer processes [1, 2] are fundamentally linked to biological ion transfer across membranes and therefore of considerable interest in analytical procedures and sensing as well as in electrocatalysis, where ion transfer is part of the overall catalytic reaction sequence [3, 4]. Selectivity in the transfer of specific anions is usually associated with ion hydrophobicity (which is related to the octanol-water partitioning constant for neutral molecules [5], but linked to a different more appropriate thermodynamic scale, the ion transfer potential [6, 7]) and/or with facilitated ion transfer [8], where reagents such as boronic acids can bind to the transferring ion at the liquid/liquid interface.

In practical laboratory experiments, the interface between the two immiscible liquids is usually defined either by liquid density (by layering the lower density liquid over the higher density liquid [9]), by micro-hole interfaces separating the two liquids [10, 11], at triple-phase boundary interfaces generated by microdroplets on the electrode surface [12, 13], or with the help of a gel [14] or organogel [15, 16] stabilizing the liquid/liquid interface. The organogel/aqueous interface is particularly convenient as it maintains shape without the need for additional substrates or density considerations. Ion transfer across this interface can be studied with a potential applied across the phase boundary. Biphasic electrocatalysis under these conditions is possible when electron transfer is coupled to ion transfer across a liquid/liquid interface [17] or across the triple-phase boundary [18]. Here, the electrochemical properties

✉ Vellaichamy Ganesan
velganesh@yahoo.com; velgan@bhu.ac.in

✉ Frank Marken
f.marken@bath.ac.uk

[1] Department of Chemistry, University of Bath, Claverton Down, Bath BA2 7AY, UK

[2] Department of Chemistry, Institute of Science, Banaras Hindu University, Varanasi 221005, India

[3] EastChem, School of Chemistry, University of Edinburgh, Joseph Black Building, David Brewster Road, Edinburgh, Scotland EH9 3FJ, UK

[4] Department of Chemistry, Swansea University, College of Science, Grove Building, Singleton Park, Swansea SA2 8PP, UK

for manganese catalysts embedded into organogel are investigated as a function of the nature of the external electrolyte.

It has recently been demonstrated that water-immiscible organic solvents such as 4-(3-phenyl-propyl)-pyridine (or PPP) can be co-deposited with a polymer of intrinsic microporosity (here PIM-EA-TB, see Fig. 1) to give organogel-like deposits at electrode surfaces [19] with good electrochemical reactivity. For example, the tetraphenylporphyrinato-Fe(III/II) (FeTPP) redox system was employed to demonstrate electron transfer coupled to anion transfer for PF_6^-, ClO_4^-, and NO_3^- at distinct transfer potentials [19]. The more hydrophobic anion, here PF_6^-, was shown to always transfer at a less positive applied potential. The possibility to form defined and electrochemically active deposits of PIM-EA-TB–PPP organogels at electrode surfaces is developed here for the case of immobilized tetraphenylporphyrinato-Mn(II) (MnTPP) and phthalocyanato-Mn(II) (MnPc) redox systems (see Fig. 1). Both the MnPc system [20] and the MnTPP system [21, 22] are of considerable interest in catalysis and surface chemistry [23] as are related poly-porphyrin-metal systems [24].

Polymers of intrinsic microporosity (or PIMs) have been developed as a new class of porous polymer materials over the past decade [25, 26]. The key feature associated with PIMs is a molecularly highly rigid polymer backbone to prevent packing and interactions. As a result, these polymers are readily soluble and film deposits remain highly porous, typically with Brunauer-Emmett-Teller (BET) surface areas of 1000 m^2 g^{-1} and a typical cumulative pore volume of 1 cm^3 g^{-1} [27]. Importantly, these polymers are highly processeable and readily applied as films to electrode surfaces [28] or to catalysts [29]. Only recently has this class of polymers been introduced to applications in electrochemistry [30]. Figure 1 shows the molecular structure of PIM-EA-TB (PIM = polymer of intrinsic microporosity, EA = ethanoanthracene, TB = Tröger base [31]), which is molecularly highly rigid and therefore highly porous. PIM-EA-TB is chloroform soluble, but insoluble in most other liquids and solvents. In a mixture with 4-(3-phenylpropyl)-pyridine (both deposited together from chloroform solution), it forms a gel-like product as a film deposit on the electrode surface. Here, Mn(II/III) metal complexes are embedded into this gel as electrochemically active chromophores. Spectroelectrochemistry is employed to follow redox state changes and associated chemical reactions in the organogel.

Both the redox active molecules (either tetraphenylporphyrinato-Mn(II) or phthalocyanato-Mn(II)) and the water-immiscible organic solvent (4-(3-phenyl-pro-pyl)-pyridine or PPP) are immobilized together with the PIM-EA-TB at glassy carbon (GC) or at porous tin-doped indium oxide (ITO) electrodes. It is shown that coupled electron transfer and anion transfer (see Fig. 1d) occur for a range of aqueous anions (as a function of anion hydrophobicity) and it is demonstrated that the PIM-EA-TB organogel can also be used on tin-doped indium oxide (ITO) electrodes to provide stable film deposits for in situ spectroelectrochemical measurements. It is concluded that MnPc exhibits a much more complex ion transfer and redox reactivity when compared to that of the chemically reversible MnTPP.
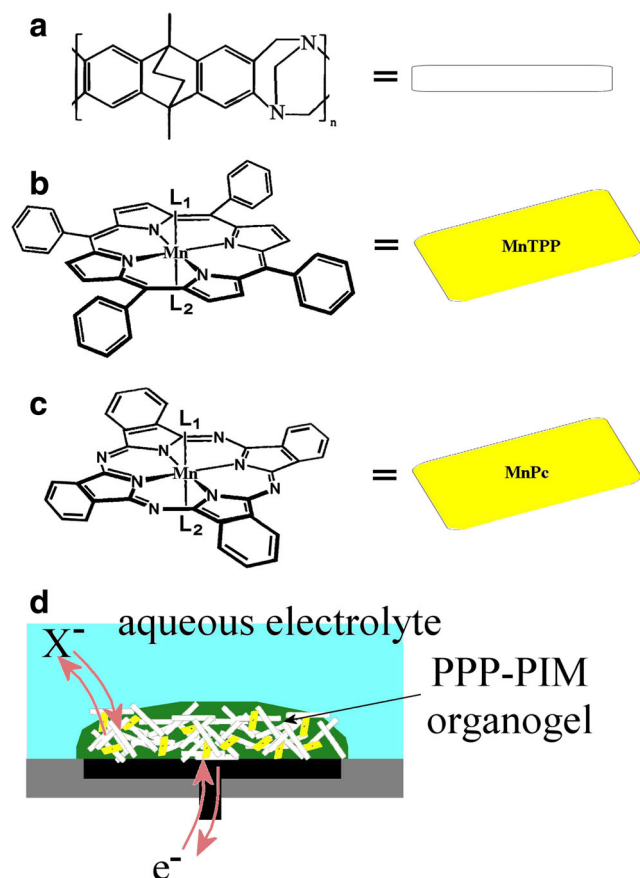

Fig. 1 Molecular structures for **a** PIM-EA-TB, **b** MnTPP, **c** MnPc, and **d** schematic drawing of an organogel deposit composed of 4-(3-phenyl-propyl)-pyridine (PPP) with PIM-EA-TB and a redox active Mn(II) complex in a coupled electron transfer with liquid/liquid anion transfer

Experimental

Chemical Reagents

N,N′-dimethylformamide (DMF), 4-(3-phenylpropyl)-pyridine) (PPP), manganese(II)-phthalocyanine (MnPc, product 379557 from Aldrich), and tetraphenylporphyrin manganese(III) chloride (MnTPP, product 254754 from Aldrich, 5,10,15,20-tetraphenyl-21H,23H-porphine manganese(III) chloride) were procured from Sigma-Aldrich and used as received. High purity $NaPF_6$, $NaClO_4$, NaCl, KF, NaSCN, Na_2SO_4, and $NaNO_3$ (Sigma-Aldrich or Fisher Scientific) were purchased and used as electrolyte in the electrochemical experiments. Indium tin oxide (ITO)-coated quartz plates were supplied with ca. 15 Ω/square from Image Optics (Basildon, UK). PIM-EA-TB was prepared following a literature procedure [31].

Instrumentation

Electrochemical experiments were carried out with a microAutolab II (Metrohm UK) potentiostat/galvanostat. A three-electrode one-compartment cell was used for all experiments. A glassy carbon electrode (GCE, BASi UK) of area 0.07 cm^2 was modified with MnPc or MnTPP organogels (with PIM-EA-TB and PPP) and employed as the working electrode. A Pt wire served as counter electrode and a KCl saturated calomel electrode (SCE) was the reference electrode. For in situ spectroelectrochemical studies, 1 cm^2 of a mesoporous ITO surface (prepared as reported previously [32]) was modified with MnPc or MnTPP organogel (with PIM-EA-TB and PPP) using drop casting. However, the amount of the coating solution was proportionately increased to maintain the organogel film thickness. Absorption spectral measurements were carried out using a Varian UV-Vis-NIR spectrophotometer. For spectroelectrochemical measurements, standard quartz cuvettes were fitted with electrodes (see below).

Procedures

Glassy carbon electrodes were cleaned by polishing on neutral alumina (0.05 μm) slurry on a Buehler microcloth pad to mirror finish followed by sonication in water and in methanol. The clean and dry electrodes were coated with 5 μL of a combined solution of (a) 2 mg/mL of MnPc or MnTPP, (b) 1 mg/mL of PIM-EA-TB (acidified with 5 μL of HClO$_4$ to aid dissolution), and (c) 10 μL/mL of PPP in DMF (note that in the final solution, all the three components were dissolved in 1 mL of DMF as per the weight/volume indicated with MnPc or MnTPP 2 mg, PIM-EA-TB 1 mg, and PPP 10 mg). The coating solution was allowed to dry at room temperature, which left a colored organogel adhered to the electrode surface. The mesoporous ITO surface was prepared by treating the ITO-coated quartz plates with ITO nanoparticles using a published procedure [33]. Aqueous solutions were prepared from purified de-ionized water collected from Thermo Scientific Ltd. water purification system (18.2 MΩcm at 22 °C). De-aeration of the electrochemical cell solution was achieved by purging 25–30 min with high purity Ar gas (BOC, Pureshield) before performing the electrochemical experiments.

Results and Discussion

Voltammetric Study of MnTPP Organogel on Glassy Carbon

A deposit of MnTPP organogel immobilized on glassy carbon was prepared based on a weight ratio of MnTPP/PIM-EA-TB/PPP of 2:1:10, that is, with an excess of 4-(3-phenyl)-pyridine as the ligand in axial position of the Mn$^{2+/3+}$ redox center in the metal complex and as the water-immiscible organogel-solvent. The resulting redox process can be described as a combined electron transfer (electrode/organogel) and anion transfer (electrolyte/organogel) as expressed in Eq. 1 [34, 35].

$$\text{MnTPP(L)}_2(\text{org}) + \text{X}^-(\text{aq}) \rightleftarrows \text{MnTPP(L)}_2{}^+(\text{org}) + \text{X}^-(\text{org}) + \text{e}^-\ (1)$$

Figure 2a shows the voltammetric responses for this system when immersed in aqueous 0.1 M NaPF$_6$. Chemically reversible voltammetric peaks for oxidation and for reduction are observed with a peak-to-peak separation close to 90 mV. The midpoint potential (here defined as $E_{mid} = ½\ E_{p,ox} + ½\ E_{p,red}$) is at $E_{mid} = -0.38$ V vs. SCE, which is indicative of a highly hydrophobic PF$_6{}^-$ anion readily transferring at relatively negative potentials into the organic phase. The effects of the amount of deposit and the concentration of gel-embedded MnTPP (nominally 280 mM) on the voltammetric response are non-trivial due to the combination of diffusion inside the gel and outside the gel. Scan rate effects are shown in Fig. 2a, but not analyzed in any further detail. In Fig. 2b, a similar data set is shown for the case of MnTPP oxidation in the presence of aqueous 0.1 M NaClO$_4$. Similar behavior is noted but with a more positive midpoint potential of $E_{mid} = -0.29$ V vs. SCE. More hydrophilic anions generally shift the midpoint potential to more positive values, and this trend continuous with 0.1 M NaSCN (Fig. 2c) and with 0.1 M NaNO$_3$ (Fig. 2d). For even more hydrophilic anions such as 0.1 M NaCl (Fig. 2e), 0.1 M KF (Fig. 2f), and 0.1 M Na$_2$SO$_4$ (Fig. 2g), the trend is less obvious. A plot of these midpoint potentials as a function of the aqueous/organic transfer potentials for anions will be shown and discussed below (vide infra). Only for very hydrophilic anions (chloride, fluoride, sulfate) the linear correlation fails. Therefore, for chloride, fluoride, and sulfate, a mechanism different to that shown in Eq. 1 needs to be assumed (possibly linked to transfer of cation/protons or hydroxide transfer in competition to electrolyte anion transfer or a process linked to competing cation transfer as noted earlier [35]).

Further aspects of anion transfer reactivity at the organogel/aqueous electrolyte interface are linked to the electrolyte concentration. Figure 2h shows data for the transfer of perchlorate anions during oxidation of MnTPP and for different concentrations of NaClO$_4$. A midpoint potential shift is observed of approximately 50–60 mV per decade change in NaClO$_4$ concentration (here 0.1 M Na$_2$SO$_4$ serves as background electrolyte) as would be expected thermodynamically [12] with lower perchlorate concentrations leading to a more positive E_{mid}

Fig. 2 a–g Cyclic voltammograms (scan rate 10, 20, 50, 100, 200 mV s^{-1}) for a deposit of MnTPP-PIM-EA-TB-PPP organogel on a 3-mm diameter glassy carbon electrode immersed into aqueous electrolyte media. h Cyclic voltammograms (scan rate 10 mV s^{-1}) obtained in 0.1 M Na$_2$SO$_4$ with 0.0, 0.01, 0.1, or 1.0 M NaClO$_4$
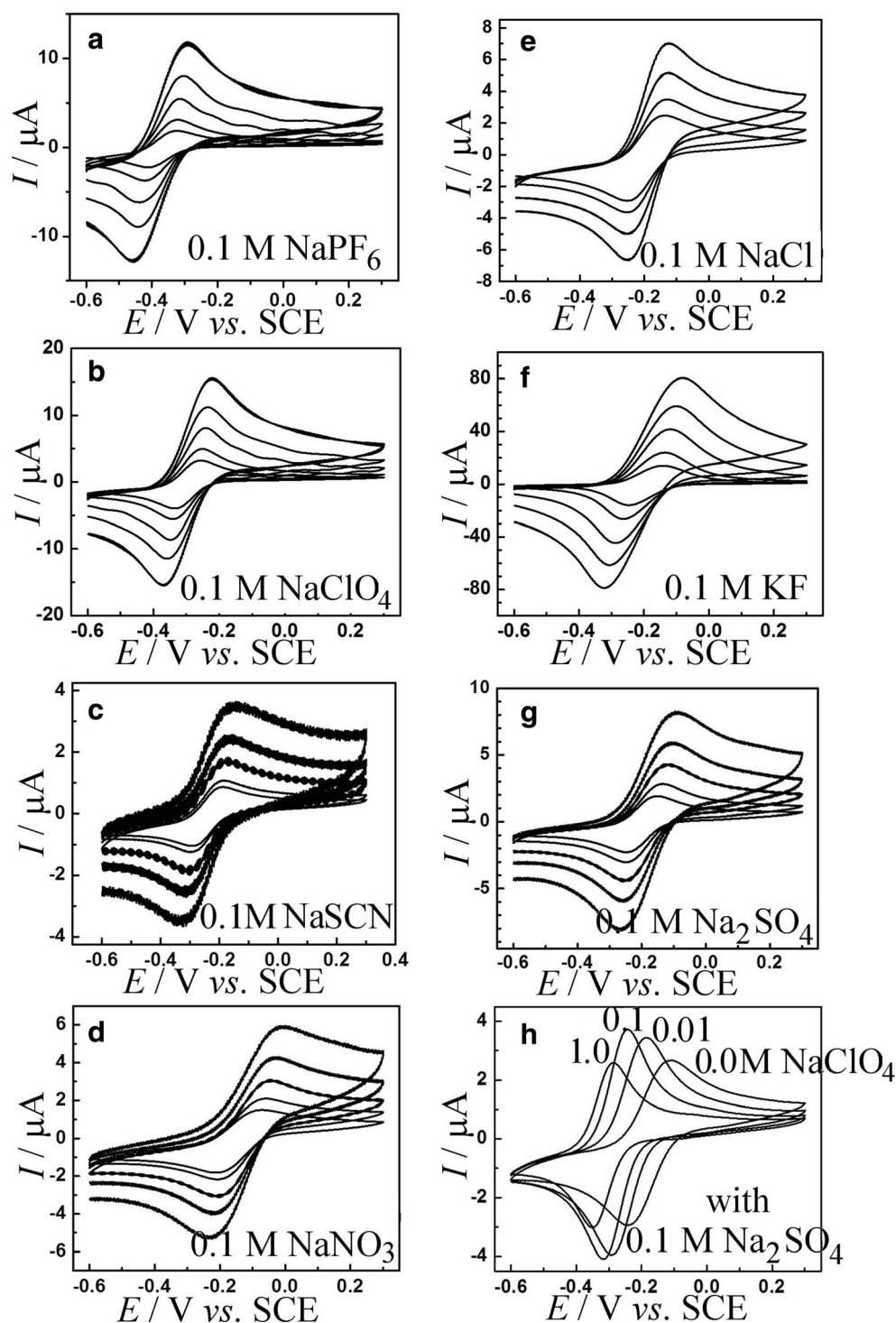
potential (finally merging with that for the sulfate transfer process). In conclusion, coupled electron and anion transfer reactions occur consistent with Eq. 1 for aqueous NaPF$_6$, NaClO$_4$, NaSCN, NaNO$_3$, but a change in reactivity is observed for the more hydrophilic anions in NaCl, KF, and Na$_2$SO$_4$. Generally, the PIM-EA-TB-PPP organogel can provide an environment for the electrochemically driven anion transfer.

Voltammetric Study of MnPc Organogel on Glassy Carbon

The MnPc redox system can be formally treated in a similar way, although the phthalocyanato macrocyclic ligand has been shown to alter the electronic structure and reactivity of the Mn metal center when compared to the phorphyrinato ligand. Based on theoretical calculations
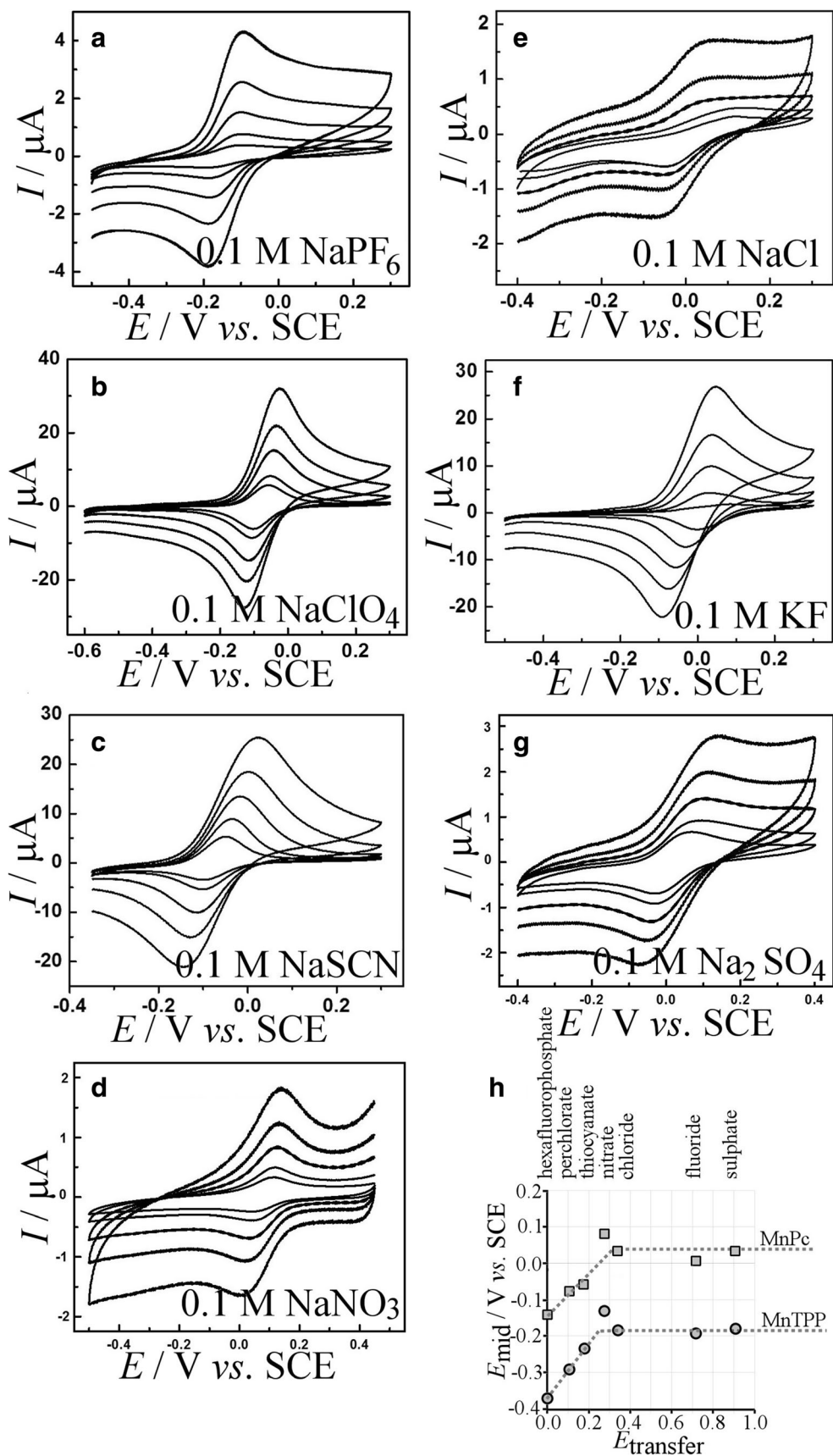
Fig. 3 **a–g** Cyclic voltammograms (scan rate 10, 20, 50, 100, 200 mV s^{-1}) for a deposit of MnPc-PIM-EA-TB-PPP organogel on a 3-mm diameter glassy carbon electrode immersed into aqueous electrolyte media. **h** Plot of midpoint potentials versus anion transfer potential

for the di-pyridine derivatives $MnPc(py)_2$ and $MnTPP(py)_2$, it has been suggested that the smaller ring size of the phthalocyanato causes a change in orbital sequence, although both Mn(II) systems should be in the same $^2A_{1g}$ electronic ground state [36]. The ionization energy for $MnPc(py)_2$ has been suggested to be about 0.42 eV higher compared to that for $MnTPP(py)_2$, although these calculations were for the parent porphyrinato and not the tetraphenylporphyrinato ligand and solvent effects were not considered. In addition, there is some uncertainty over the true nature of these complexes as being mono- or di-pyridine axially ligated in the ground state. Equation 2 describes the anticipated (simplified) Mn(III/II) reaction during combined electron transfer and anion transfer for the MnPc-PIM-EA-TB-PPP organogel deposit on a glassy carbon electrode.

$$MnPc(L)_2(org) + X^-(aq) \rightleftarrows MnPc(L)_2^+(org) + X^-(org) + e^- \quad (2)$$

Data in Fig. 3 confirm the coupled electron and anion transfer. Figure 3a shows cyclic voltammograms for different scan rates and for the transfer of aqueous PF_6^- into the organogel phase. The midpoint potential is determined as $E_{mid} = -0.13$ V vs. SCE, which is shifted positive when compared to the corresponding process for MnTPP and broadly consistent with literature reports [37]. This shift in potential (ca. 0.23 V) is consistent with the predicted increase in ionization energy for the phthalocyanato ligand when compared to the tetraphenylphorphyrinato ligand

[37]. When investigating aqueous electrolyte media with $NaClO_4$, NaSCN, and $NaNO_3$ (see Fig. 3b–d), the anticipated trend to more positive E_{mid} potentials is seen. For more hydrophilic anions (NaCl, KF, Na_2SO_4 in Fig. 3e–g), a switch in anion transfer mechanism is indicated by the change in midpoint potential trend. Figure 3h shows a plot summarizing all trends in midpoint potentials. Table 1 provides a summary of data from voltammetric experiments including peak potentials and midpoint potentials.

Spectroelectrochemical Study of MnTPP or MnPc Organogels on ITO

In order to gain further information about the coupled electron transfer and anion transfer mechanism, additional spectroelectrochemical measurements were performed employing transparent tin-doped indium oxide (ITO) electrodes that were coated with ITO nanoparticles. This type of partially transparent porous electrode has been shown previously to allow electron transfer coupled to ion transfer under conditions of spectroelectrochemistry [32]. Spectroelectrochemical properties of Mn(II/III)TPP systems are of interest and are non-trivial in terms of axial ligand affecting redox and electronic states [38]. Schultz and coworkers demonstrate that the Soret-Q bands for Mn(II) and Mn(III) complexes are indicators of structural changes such as solvent ligand attachment. For solvent of high Gutman donor number [39], the species $Mn(II/III)TPP(L)_2^{0/+}$ was suggested to be dominant associated with a strong decrease in Soret-Q band intensity during oxidation from Mn(II) to Mn(III).

Table 1 Data summary for cyclic voltammetry experiments (scan rate 20 mV s^{-1}, in argon-saturated solution) for a deposit of MnPc/MnTPP-PIM-EA-TB-PPP organogel on a 3-mm diameter glassy carbon electrode immersed into aqueous electrolyte media

Electrode	$E_{p,a}$/mV vs. SCE	$E_{p,c}$/mV vs. SCE	E_{mid}/V vs. SCE	Electrolyte
GC/MnTPP-PIM-EA-TB-PPP organogel	−323	−423	−0.373	0.1 M NaPF$_6$
	−254	−339	−0.296	0.1 M NaClO$_4$
	−187	−291	−0.239	0.1 M NaSCN
	−63	−199	−0.131	0.1 M NaNO$_3$
	−127	−251	−0.189	0.1 M NaCl
	−135	−266	−0.200	0.1 M KF
	−120	−238	−0.179	0.1 M Na$_2$SO$_4$
	−183	−289	−0.236	0.1 M Na$_2$SO$_4$ + 0.01 M NaClO$_4$
	−242	−317	−0.280	0.1 M Na$_2$SO$_4$ + 0.1 M NaClO$_4$
	−287	−350	−0.318	0.1 M Na$_2$SO$_4$ + 1 M NaClO$_4$
GC/MnPC-PIM-EA-TB-PPP organogel	−98	−188	−0.143	0.1 M NaPF$_6$
	−52	−106	−0.079	0.1 M NaClO$_4$
	−36	−100	−0.068	0.1 M NaSCN
	118	43	0.081	0.1 M NaNO$_3$
	+116	−46	0.035	0.1 M NaCl
	+33	−34	0.0	0.1 M KF
	+94	+26	0.034	0.1 M Na$_2$SO$_4$

Figure 4a shows spectral data in the wavelength range from 300 to 1000 nm for a MnTPP-PIM-EA-TB-PPP organogel deposit immersed in aqueous 0.1 M NaClO$_4$. Seven potentials are applied sequentially (see inset) to investigate the transition from Mn(II) to Mn(III). A very strong Soret band at 442 nm is consistent with the reduced Mn(II)TPP(L)$_2$ metal complex. At an applied potential of − 0.4 V vs. SCE, a transition occurs with the main band at 442 nm diminishing and a new band at

472 nm appearing consistent with a previous report [32]. The new band is consistent with the Mn(III)TPP(L)$_2$ metal complex, which has a Soret band at longer wave length and with considerably lower extinction coefficient. The mechanism can be confirmed (tentatively) as electron transfer coupled to anion transfer (see Eq. 1).

Table 2 summarizes spectral data obtained in aqueous 0.1 M NaSCN, 0.1 M NaNO$_3$, and in 0.1 M KF. In all cases,

Fig. 4 Spectroelectrochemical data for **a** MnTPP-PIM-EA-TB-PPP organogel immobilized onto porous ITO and immersed into aqueous 0.1 M NaClO$_4$, **b** MnPc-PIM-EA-TB-PPP organogel immobilized onto porous ITO and immersed into aqueous 0.1 M NaClO$_4$, and **c** as in **b** but stepping the applied voltage from (i) 0.5 to (ii) -0.6 to (iii) 0.5 to (iv) − 0.6 V vs. SCE demonstrating the loss of the absorption band at 720 nm
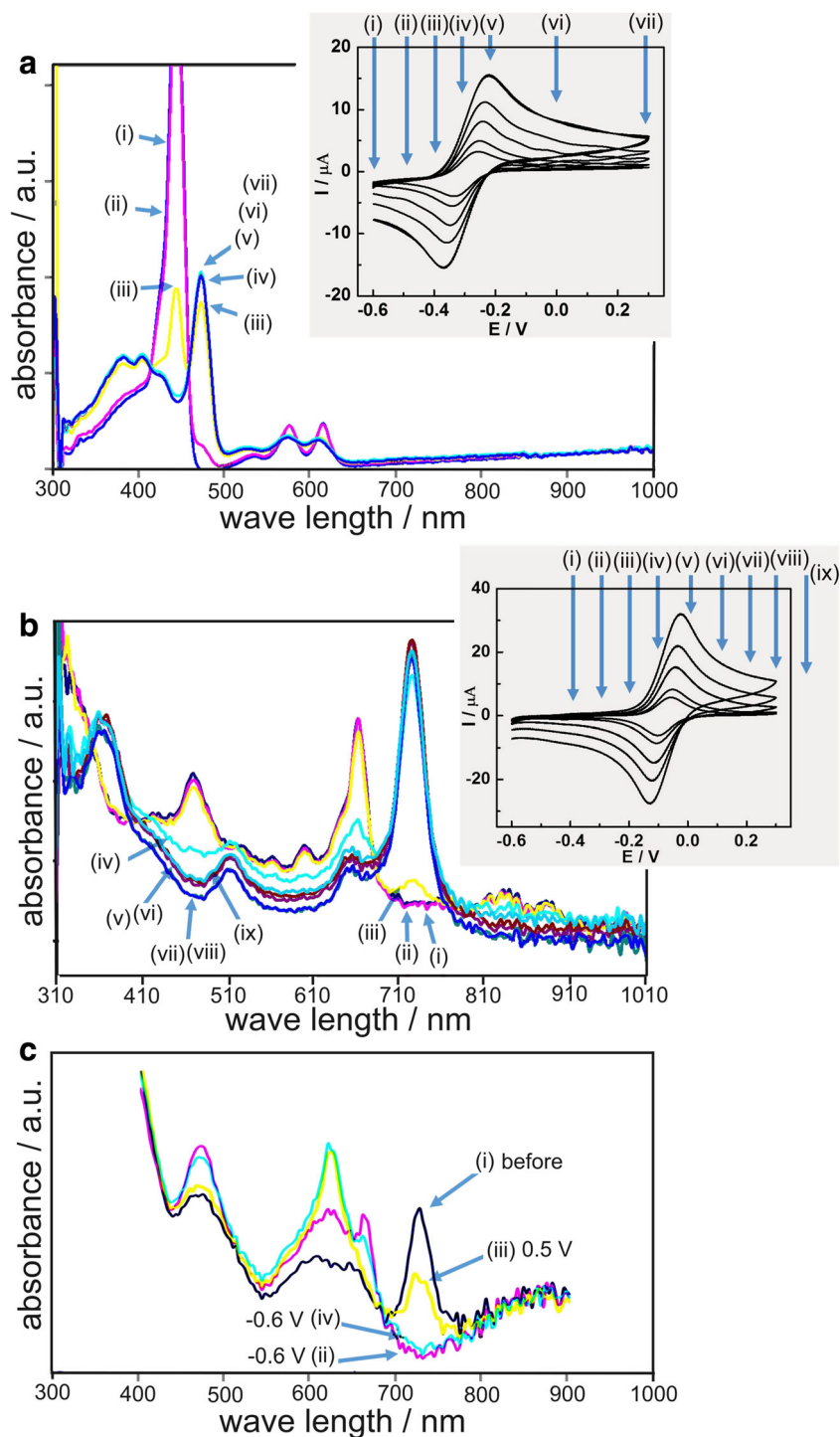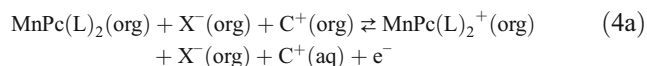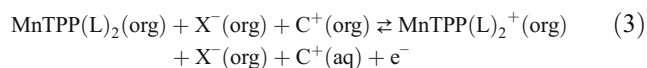
Table 2 Summary of UV/Vis spectroelectrochemical data indicating the λ_{max} values for reduced (-0.6 V vs. SCE) and oxidized ($+0.3$ V vs. SCE) forms of MnPc and MnTPP obtained in organogel biphasic media on mesoporous ITO electrodes in the presence of different types of aqueous electrolyte

	λmax (reduced -0.6 V vs. SCE)	λmax (oxidized $+0.3$ V vs. SCE)	Conditions
MnTPP with PIM and PPP on ITO nanoparticles coated ITO electrode	442 nm	472 nm	0.1 M NaClO$_4$ (presence of O$_2$ or absence of O$_2$ makes no difference)
	445 nm	469 nm	0.1 M NaNO$_3$ (in presence of O$_2$)
	449 nm	480 nm	0.1 M KF (in presence of O$_2$)
	445 nm	475 nm	0.1 M NaSCN (in presence of O$_2$)
MnPc with PIM and PPP on ITO nanoparticles coated ITO electrode	663 nm	726 nm	0.1 M NaClO$_4$ (in absence of O$_2$)
	620 nm (663 nm peak appears, however then disappears)	720 nm	0.1 M NaClO$_4$ (in presence of O$_2$)
	620 nm (663 nm peak appears, however then disappears)	720 nm	0.1 M NaNO$_3$ (in absence of O$_2$)
	623 nm	663 nm	0.1 M KF (in absence of O$_2$)
	663 nm	723 nm	0.1 M NaSCN (in absence of O$_2$)

a similar pattern is observed of the Soret band shifting upon oxidation by approximately 30 nm. Therefore, even for the highly hydrophilic anions (such as fluoride), a similar mechanism has to be assumed in spite of the midpoint potential indicating a change in mechanism. In earlier work [32], more complex behavior was observed in the presence of fluoride and the change to the chemically more reversible behavior observed here has to be attributed to the presence of PM-EA-TB as a hydrophobic environment stabilizing the system. Equation 3 describes a hypothetical process assuming the transfer of the cation to balance the charge after/during electron transfer. However, the alternative transfer of hydroxide (or proton expulsion) is also possible.

$$MnTPP(L)_2(org) + X^-(org) + C^+(org) \rightleftarrows MnTPP(L)_2^+(org) \quad (3)$$
$$+ X^-(org) + C^+(aq) + e^-$$

$$MnPc(L)_2(org) + X^-(org) + C^+(org) \rightleftarrows MnPc(L)_2^+(org) \quad (4a)$$
$$+ X^-(org) + C^+(aq) + e^-$$

$$MnPc(L)X^-(org) + C^+(org) \rightleftarrows MnPc(L)_2X(org) + C^+(aq) + e^- \quad (4b)$$

A similar pattern of behavior is observed for Mn(II)Pc oxidation to Mn(III)Pc. Data in Fig. 4b show spectral changes for nine potential steps with the Soret band shifting from 663 nm (reduced form) to 726 nm (oxidized form) consistent with literature reports [40]. A similar mechanism (Eq. 4a) can be postulated, but the MnPc system seems more complex and chemically more active under these conditions. When switching from reduced to oxidized state in the presence of NaClO$_4$, multiple reversible redox state switching is possible under an argon atmosphere. In the presence of more hydrophilic electrolyte such as KF, a new pair of Soret peaks occurs at 623 nm (reduced form) and at 663 nm (oxidized form) consistent with a substitution on the metal center. For aqueous 0.1 M NaSCN and 0.1 M NaNO$_3$, similar changes

in peak pattern occur but more slowly. Finally, for all MnPc spectroelectrochemical measurements, a new phenomenon was observed in the presence of ambient levels of oxygen. Figure 4c shows how the Soret peak at 663 nm is rapidly lost first to give the 720 nm band for the oxidized material, but then giving a broad band at 620 nm. This broad band at 620 nm appears to remain associated with a material that is electrochemically inactive. A similar observation has previously been linked to the formation of an oxygen complex [41] or oxygen-bridged dimeric species (see Eq. 5 [42, 43]). The observation that the Soret band is lost in Fig. 4c may suggest further reaction steps that ultimately lead to the loss of the electrochemical signal.

$$2\,MnPc(L)_2(org) + O_2(org) \rightleftarrows (L)PcMn-O_2-MnPc(L)(org) + 2\,L(org) \quad (5)$$

A summary of spectroelectrochemical data for MnTPP and MnPc organogel immobilized on mesoporous ITO and in contact to different types of aqueous electrolyte is provided in Table 2. For MnTPP organogel materials, the redox state switching occurs over multiple cycles and without loss of activity even in the presence of ambient levels of oxygen. For MnPc organogels, the redox state switching occurs in the presence of both hydrophobic and hydrophilic electrolyte anions; however, changes in the wavelength for Soret bands may suggest complexity and ligand exchange as well as sensitivity towards the presence of ambient oxygen. More work will be required to provide further detail and a better resolved description of these types of processes.

Conclusions

It has been shown that PIM-EA-TB can be employed to form organogel deposits for anion transfer voltammetry at PPP/aqueous electrolyte interfaces. For two redox systems,

MnTPP and MnPc, and for a range of electrolyte anions, chemically reversible voltammetric responses were obtained. The correlation of anion transfer potential to midpoint potential suggests that for PF_6^-, ClO_4^-, SCN^-, and for NO_3^- anion transfer is linked to Mn(II/III) oxidation. A midpoint potential shift of 0.23 V positive when going from MnTPP to MnPc has been attributed to an electronic effect of the macrocyclic ligand. However, for more hydrophilic Cl^-, F^-, SO_4^{2-}, anion additional processes possibly linked to competing cation transfer or to hydroxide transfer cannot be ruled out. The level of complexity is higher for MnPc, where also additional effects from the presence of ambient oxygen are observed.

PIM-EA-TB in the organogel has been suggested to have a stabilizing role in providing a microporous environment to bind hydrophobic solvent molecules such as PPP. The organogel deposits are readily formed at glassy carbon or on mesoporous ITO electrode surfaces. Spectroelectrochemical data confirmed the chemically reversible transfer of anions in particular for MnTPP. However, for MnPc and in the presence of either hydrophilic anions or ambient oxygen, an additional "loss mechanism" occurs leading probably to oxygen-bound monomeric or oxygen-bridged dimeric products and follow on processes that lead to products without electrochemical signature. In the future, PIM-EA-TB organogels can be employed to define liquid/liquid interfaces or triple-phase boundary redox processes for both voltammetry (with sensor or catalysis applications) or for spectro-electrochemistry to better define and understand coupled electron-transfer ion-transfer reactivity at the liquid/liquid boundary.

References

1. H.H.J. Girault, D.J. Schiffrin, Electroanal. Chem. **15**(1) (1989)
2. C.E. Banks, T.J. Davies, R.G. Evans, G. Hignett, A.J. Wain, N.S. Lawrence, J.D. Wadhawan, F. Marken, R.G. Compton, Electrochemistry of immobilised redox droplets: Concepts and applications. Phys. Chem. Chem. Phys. **5**(19), 4053 (2003)
3. Y.H. Shao, M.V. Mirkin, J.F. Rusling, J. Phys. Chem. B **101**, 3202 (1997)
4. T.R. Bartlett, S. Ahmed, F. Tuna, D. Collison, G.J. Blanchard, F. Marken, Liquid|Liquid Interfacial Photoelectrochemistry of Chromoionophore I Immobilised in 4-(3-Phenylpropyl)Pyridine Microdroplets. ChemElectroChem **1**(2), 400–406 (2014)
5. G. Bouchard, A. Galland, P.A. Carrupt, R. Gulaboski, V. Mirceski, F. Scholz, H.H. Girault, Phys. Chem. Chem. Phys. **5**, 3748 (2003)
6. Y. Marcus, *Ion Properties* (Marcel Dekker, New York, USA, 1997)
7. S.M. MacDonald, M. Opallo, A. Klamt, F. Eckert, F. Marken, Probing carboxylate Gibbs transfer energies via liquid|liquid transfer at triple phase boundary electrodes: ion-transfer voltammetry versus COSMO-RS predictions. Phys. Chem. Chem. Phys. **10**(26), 3925–3933 (2008)
8. M. Li, G.E.M. Lewis, T.D. James, Y.T. Long, B. Kasprzyk-Hordern, J.M. Mitchels, F. Marken, Oil|Water Interfacial Phosphate Transfer Facilitated by Boronic Acid: Observation of Unusually Fast Oil|Water Lateral Charge Transport. ChemElectroChem **1**(10), 1640–1646 (2014)
9. A. Martinez, A. Colina, R.A.W. Dryfe, V. Ruiz, Electrochim. Acta, **54**, 5071 (2009)
10. P.D. Beattie, A. Delay, H.H. Girault, Electrochim Acta, **40**, 2961 (1995)
11. A.J. Olaya, M.A. Mendez, F. Cortes-Salazar, H.H. Girault, J. Electroanal. Chem. **644**, 60 (2010)
12. F. Marken, J.D. Watkins, A.M. Collins, Phys. Chem, Chem. Phys. **13**, 10036 (2011)
13. A.M. Collins, G.J. Blanchard, J. Hawkett, D. Collison, F. Marken, Liquid|Liquid|Electrode Triple-Phase Boundary Photovoltammetry of Pentoxyresorufin in 4-(3-Phenylpropyl)pyridine. Langmuir **27**(10), 6471–6477 (2011)
14. B.M.B. Felisilda, E.A. de Eulate, D.W.M. Arrigan, Anal Chim. Acta **893**, 34 (2015)
15. M.M. Hossain, H.H. Girault, H.J. Lee, Bull Korean Chem Soc **33**, 1734 (2012)
16. M.D. Scanlon, J. Strutwolf, A. Blake, D. Iacopino, A.J. Quinn, D.W.M. Arrigan, Anal. Chem. **82**, 6115 (2010)
17. R.M. Lahtinen, D.J. Fermin, H. Jensen, K. Kontturi, H.H. Girault, Electrochem Commun **2**, 230 (2000)
18. J.D. Wadhawan, A.J. Wain, A.N. Kirkham, D.J. Walton, B. Wood, R.R. France, S.D. Bull, R.G. Compton, Electrocatalytic Reactions Mediated byN,N,N',N'-Tetraalkyl-1,4-phenylenediamine Redox Liquid Microdroplet-Modified Electrodes: Chemical and Photochemical Reactions In, and At the Surface of, Femtoliter Droplets. J. Amer. Chem. Soc. **125**(37), 11418–11429 (2003)
19. Y.Y. Rong, R. Malpass-Evans, M. Carta, N.B. McKeown, G.A. Attard, F. Marken, Electrochem. Commun. **46**(26) (2014)
20. J.D. Blakemore, J.F. Hull, R.H. Crabtree, G.W. Brudvig, Dalton Trans **41**, 7681 (2012)
21. Z. Solati, M. Hashemi, A. Keshavarzi, E. Rafiee, J Porph Phthaloc **16**, 149 (2012)
22. S.D. Ahn, B. Mao, S.I. Pascu, A. Vuorema, J. Mitchels, F. Marken, Electroanalysis **26**, 69 (2014)
23. J.M. Gottfried, Surf. Sci. Rep. **70**, 259 (2015)
24. D.V. Konev, O.I. Istakova, B. Dembinska, M. Skunik-Nuckowska, C.H. Devillers, O. Heintz, P.J. Kulesza, M.A. Vorotyntsev, Electrocatalytic properties of manganese and cobalt polyporphine films toward oxygen reduction reaction. J. Electroanal. Chem. **816**, 83–91 (2018)
25. P.M. Budd, B.S. Ghanem, S. Makhseed, N.B. McKeown, K.J. Msayib, C.E. Tattershall, Polymers of intrinsic microporosity (PIMs): robust, solution-processable, organic nanoporous materials. Chem. Commun. (2), 230–231 (2004)
26. N.B. McKeown, P.M. Budd, Exploitation of Intrinsic Microporosity in Polymer-Based Materials. Macromol. **43**(12), 5163–5176 (2010)
27. E. Madrid, Y.Y. Rong, M. Carta, N.B. McKeown, R. Malpass-Evans, G.A. Attard, T.J. Clarke, S.H. Taylor, Y.T. Long, F. Marken, Angew. Chem. Inter. Ed. **53**, 10751 (2014)
28. A. Kolodziej, S.D. Ahn, M. Carta, R. Malpass-Evans, N.B. McKeown, R.S.L. Chapman, S.D. Bull, F. Marken, Electrochim. Acta 160, 195 (2015)

29. D.P. He, Y.Y. Rong, Z.K. Kou, S.C. Mu, T. Peng, R. Malpass-Evans, M. Carta, N.B. McKeown, F. Marken, Electrochem. Commun. **59**, 72 (2015)

30. E. Madrid, N.B. McKeown, Curr Opinion Electrochem (2018). https://doi.org/10.1016/j.coelec.2018.04.008

31. M. Carta, R. Malpass-Evans, M. Croad, Y. Rogan, J.C. Jansen, P. Bernardo, F. Bazzarelli, N.B. McKeown, An Efficient Polymer Molecular Sieve for Membrane Gas Separations. Science **339**(6117), 303–307 (2013)

32. A. M. Collins, G. J. Blanchard, F, Marken, Electroanalysis **24**, 246 (2012)

33. J. Niedziolka, K. Szot, F. Marken, M. Opallo, A Porous ITO Nanoparticles Modified Electrode for the Redox Liquid Immobilization. Electroanalysis **19**(2-3), 155–160 (2007)

34. M.A. Ghanem, F. Marken, Electrochem. Commun. **7**, 1333 (2005)

35. M.J. Bonné, C. Reynolds, S. Yates, G. Shul, J. Niedziolka, M. Opallo, F. Marken, The electrochemical ion-transfer reactivity of porphyrinato metal complexes in 4-(3-phenylpropyl)pyridine | water systems. New J. Chem. **30**(3), 327 (2006)

36. M.S. Liao, J.D. Watts, M.J. Huang, Inorg Chem **44**, 1941 (2005)

37. A.B.P. Lever, P.C. Minor, J.P. Wilshire, Inorg Chem **20**, 2550 (1981)

38. X.H. Mui, F.A. Schultz, Inorg. Chem. **34**, 3835 (1995)

39. V. Gutmann, *The Donor-Acceptor Approach to Molecular Interactions* (Plenum Press, New York, 1978)

40. G. Ricciardi, A. Bavoso, A. Bencini, A. Rosa, F. Lelj, F. Bonosi, Synthesis, structure, magnetic, spectroscopic and electrochemical behaviour of chloro-iron(III) and -manganese(III) complexes of 2,3,7,8,12,13,17,18-octakis(ethylsulfanyl)-5,10,15,20-tetraazaporphyrin. J. Chem. Soc. Dalton Trans. (13), 2799 (1996)

41. A.B.P. Lever, J.P. Wilshire, S.K. Quan, J. Amer. Chem. Soc. **101**, 3668 (1979)

42. N.T. Moxon, P.E. Fielding, A.K. Gregson, J. Chem. Soc. Chem. Commun., 98 (1981)

43. T. Watanabe, T. Ama, K. Nakamoto, Inorg. Chem. **22**, 2470 (1983)